JACS
JOURNAL OF THE AMERICAN CHEMICAL SOCIETY

Article

pubs.acs.org/JACS

Water Sensitivity in Zn_4O-Based MOFs is Structure and History Dependent

Ping Guo,[†] Dhanadeep Dutta,[‡,§] Antek G. Wong-Foy,[†] David W. Gidley,*[,‡] and Adam J. Matzger*[,†]

[†]Department of Chemistry, University of Michigan, 930 N. University, Ann Arbor, Michigan 48109-1055, United States
[‡]Department of Physics, University of Michigan, 450 Church Street, Ann Arbor, Michigan 48109-1040, United States

Supporting Information

ABSTRACT: Moisture can cause irreversible structural collapse in metal-organic frameworks (MOFs) resulting in decreased internal surface areas and pore volumes. The details of such structural collapse with regard to pore size evolution during degradation are currently unknown due to a lack of suitable *in situ* probes of porosity. Here we acquire MOF porosity data under dynamic conditions by incorporating a flow-through system in tandem with positronium annihilation lifetime spectroscopy (PALS). From the decrease in porosity, we have observed an induction period for water degradation of some Zn_4O-based MOFs that signals much greater stability than commonly believed to be possible. The sigmoidal trend in the degradation curve of unfunctionalized MOFs caused by water vapor has been established from the temporal component of pore size evolution as characterized by *in situ* PALS. IRMOF-3 is found to degrade at a lower relative humidity than MOF-5, a likely consequence of the amine groups in the structure, although, in contrast to MOF-5, residual porosity remains. The presence of an induction period, which itself depends on previous water exposure of the sample (history dependence), and sigmoidal temporal behavior of the moisture-induced degradation mechanism of MOFs was also verified using powder X-ray diffraction analysis and *ex situ* gas adsorption measurements. Our work provides insight into porosity evolution under application-relevant conditions as well as identifying chemical and structural characteristics influencing stability.

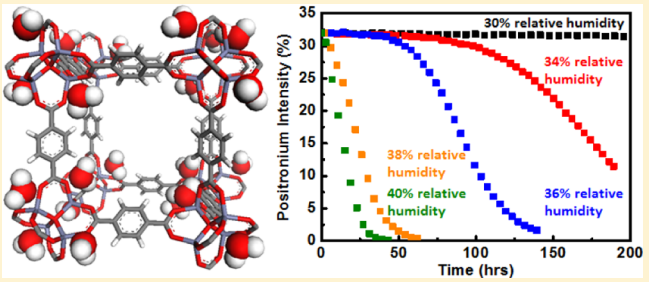

INTRODUCTION

Metal-organic frameworks (MOFs) have attracted broad interest from scientists and engineers because their porosity is often maintained in the absence of guests. Furthermore, their regular and controllable crystalline structure offers a level of control over both chemical functionality and pore geometry. Thus, MOFs have been investigated as candidates for applications such as H_2 storage,[1−4] CO_2 capture,[5−9] liquid phase separations,[10−12] and catalysis.[13] Commercial applications of MOFs have been slow to develop, and one often cited barrier to applications for some of the earliest and most extensively studied classes of MOFs is their instability against moisture.[14] Tremendous advances have been made toward the goal of water-stable/water-resistant MOFs, and these advances have primarily been realized by changing the nature of the metal-linker interaction.[15−20]

The degradation of some MOFs caused by water has been monitored by powder X-ray diffraction (PXRD),[21,22] post-exposure gas sorption analysis,[14,15] and optical microscopy.[23] For example, a PXRD study of the structural integrity of a variety of MOFs exposed to various concentrations of water in organic solvent led to the conclusion that one of the decisive factors in determining water stability of MOFs is their metal clusters.[21] MOFs with $Zn_4O(CO_2R)_6$ metal clusters are less water stable compared to the ones with copper paddlewheel clusters followed by those with trinuclear chromium clusters; this ordering is in general accord with computational predictions from quantum mechanical calculations based upon cluster models.[22] Water stability of MOFs has also been proposed to be influenced by many factors such as the number of metal ions in the cluster, oxidation state of the metals, and metal−oxygen bond strength in the corresponding metal oxides.[22] The effect of linker functionality on MOF humidity stability has received considerable attention.[24] The MOF often becomes less sensitive to moisture when hydrophobic functional groups are incorporated.[25−27] Even though the structure dependence of MOF water sensitivity/stability is known in the MOF community, MOF water sensitivity/stability is normally treated as a binary phenomenon: the discussed MOF is either water stable or unstable. This is partially because of a critical shortcoming with the previous studies that the techniques applied so far offer limited understanding of the interaction between water and MOFs. PXRD gives averaged information about bulk crystallinity but offers little information on disorder; gas sorption analysis can quantitatively measure the accessible internal surface area, but no information on local disorder or porosity inaccessible to the probe gas is obtained. Most

Received: December 4, 2014
Published: February 2, 2015

DOI: 10.1021/ja512382f
J. Am. Chem. Soc. 2015, 137, 2651−2657

importantly, neither of these techniques can characterize disorder and monitor pore structural changes during adsorption in real-time. PXRD is known to sometimes predict high porosity when none is observed,[28] and sorption analysis requires halting water exposure and re-evacuating the sample prior to analysis. In other words, the two central techniques for understanding porosity changes upon water exposure are fundamentally inadequate. Here we overcome many of these limitations by utilizing a complementary technique, positronium annihilation lifetime spectroscopy (PALS), integrated into a gas flow-through system (Figure S1). Striking results have been found that suggest wide regions of exceptional stability even for those materials previously considered to be quite sensitive. In particular the focus of this study is MOFs based on the Zn_4O cluster and their water induced degradation as a function of time and relative humidity. $Zn_4O(FMA)_3$,[29] MOF-5,[30] UMCM-8,[31] and IRMOF-3[32] are found to be stable under a certain range of relative humidities for extended time periods and display stabilities depending on structure and history not possible to rationalize solely from the chemistry of the isolated metal cluster (Figure 1).

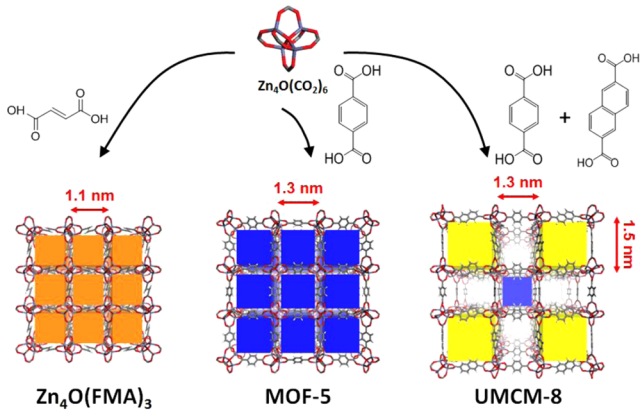

Figure 1. Compositions and structure comparison of $Zn_4O(FMA)_3$ ($Zn_4O(fumarate)_3$), MOF-5 ($Zn_4O(benzene\text{-}1,4\text{-}dicarboxylate)_3$), and UMCM-8 ($Zn_4O(benzene\text{-}1,4\text{-}dicarboxylate)_{1.5}(naphthalene\text{-}2,6\text{-}dicarboxylate)_{1.5}$). The accessible cubic pore spaces are depicted by colored cubes. The cage metrics are marked accordingly.

PALS has been utilized as a probe for vacancies and pores in crystalline and amorphous materials for over 40 years.[33,34] However, PALS is quite new to the MOF field, with only a few examples[35,36] validating it as an *in situ* nondestructive technique complementing the traditional probes for MOFs. Characterization of inaccessible pore space,[28] structural evolution in MOFs during heating,[35] porosity information on MOFs during gas adsorption[35,36] have all been successfully studied. Since the positronium (Ps) annihilation lifetime in porous materials can be reliably correlated to the pore diameter using the Tao–Eldrup model[33,37,38] (Figure S2), PALS is an ideal technique to characterize changes in pore size or pore size distribution due to degradation by water. Water vapor can break down the coordination bonds in MOFs leading to local framework collapse.[39] As a result, the relative amount of intact framework pores will be reduced, and this can be detected in the PALS spectrum as a decrease in the intensity of Ps annihilating in the framework pores (Ps with the characteristic framework lifetime). Therefore, PALS is well suited to monitor pore evolution of MOFs in real-time under humid conditions.

RESULTS AND DISCUSSION

MOF-5[30] is one of the first exceptionally high surface area MOFs, and we have utilized it as the benchmark material for a variety of applications.[10,40,41] It has been studied in detail and is reported to be very sensitive to water vapor.[21,42−45] The performance of MOF-5 is compromised by its sensitivity to water vapor.[42−46] We have previously reported that MOF-5 maintains its crystallinity after soaking in a mixture of water and DMF in the ratio of 1:8 for 1 h.[21] Another study has claimed that MOF-5 was observed to decompose in humid air in as short as 10 min (relative humidity not reported).[47] This ambiguity motivates developing a better quantitative understanding of the porosity evolution of MOF-5 caused by its interaction with water.

PALS was applied to MOF crystals under controlled relative humidity. MOF crystals were placed in a 0.29 cm^3 well within an aluminum sample holder having a horizontal bore to allow gas flow through the sample (Figure 2). For a general PALS-

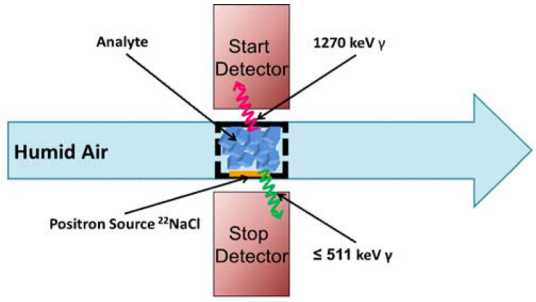

Figure 2. Illustration of the flow-through PALS apparatus.

hydration experiment, ~80, ~80, ~30, and ~100 mg were loaded in the sample holder for MOF-5, UMCM-8, $Zn_4O(FMA)_3$, and IRMOF-3, respectively. The sample holder was sealed by an aluminum lid to allow loading of the MOF in the glovebox and eliminate interaction with the atmosphere. The positron source, $^{22}NaCl$, enclosed in a 13 μm thick Kapton film, was attached to the lid and placed adjacent to the sample. The sample holder was flipped upside down so that the sample was as close to the source as possible to maximize positrons stopping in the MOF. A nitrogen flow at 20 mL/min with controlled relative humidity was achieved by mixing dry nitrogen (0% relative humidity) and humid nitrogen (100% relative humidity, generated from an 80 cm height column of water with gas dispersion tube) with controlled flow rates (Figure S1). Nitrogen was used in preference to air because oxygen is paramagnetic resulting in spin quenching that reduces the Ps lifetime in air to about 70 ns compared to 138 ns in nitrogen at 1 atm. Humidity sensors were placed before and after the sample holder to monitor the inlet and outlet gas stream. Two fast plastic gamma detectors, 5.08 cm in diameter, were placed closely above and below the sample holder as start and stop detectors. The 1270 keV gamma ray coincident with beta emission from ^{22}Na is monitored by the start detector as the start signal of the production of a positron. The subsequent annihilation of Ps generates gamma ray photons (≤511 keV) which can be detected by the stop detector. The lifetime of the Ps event is the time interval between the start and stop signals.[33] The Ps lifetime spectrum is a histogram of several million of such lifetime measurements (Figure S3). This spectrum is fitted to a sum of exponentially decaying

DOI: 10.1021/ja512382f
J. Am. Chem. Soc. 2015, 137, 2651−2657

components characterized by a pore-sensing Ps lifetime in ns and its corresponding intensity (the fraction of all positrons that decay as Ps with the corresponding lifetime). A second Ps component with a lifetime around 138 ns (characteristic of Ps decaying in 1 atm of N_2) accounts for Ps that has diffused out of the MOF grain and annihilates in the intergranular gas-filled space. We also search for the presence of any other Ps lifetimes that may emerge as a result of framework collapse and/or void coalescence. With a specific relative humidity setting, one PALS spectrum is collected every 4 h in automated scans that range from typically 2 days to 2 weeks. The lifetime (ns) of Ps decaying in the MOF framework pores (hereafter referred to as Ps framework lifetime) and the intensity (in %) of the Ps with that lifetime (hereafter referred to as Ps framework intensity) are fitted from each spectrum and then plotted against time (hours) of humid nitrogen exposure.

When a steady nitrogen flow at 20 mL/min with 40% relative humidity at 25 °C is flowed through a bed of ~80 mg MOF-5, the Ps framework lifetime (representing the size of framework pores) decreases from 13.0 to 12.4 ns within the first 19 h (green symbols in Figure S4). This slight decrease in Ps framework lifetime is consistent with some minimal accumulation of water molecules in the pores prior to their collapse, While the intensity of framework Ps, which indicates the relative population of intact framework pores in the material, decreases from 32% to 9%. This indicates that the typical MOF-5 crystals have only 28% of its original porosity remaining after 19 h exposure to 40% relative humidity. The decrease in both Ps framework lifetime and Ps intensity correlates with the structural rearrangement/degradation of MOF-5. After the initial slight decrease, the Ps framework lifetime dramatically drops from 12.4 to 6.3 ns with wider error bars of ±2.1 ns, and the Ps intensity keeps going downward from 9% to 0.15%, indicating that the MOF-5 framework collapses catastrophically. Based on the correlation between Ps framework lifetime (ns) and cubic pore diameter (nm) (Figure S2), the aforementioned lifetime drop suggests that 40% relative humidity causes the size of MOF-5 framework cell to change from a uniform 1.3 nm to a collection of different sizes ranging from 1.02 to 0.69 nm at the end of the experiment. The decrease of the framework intensity from 32% down to 0.15% is due to irreversible local cell collapse instead of water condensing and filling the cells based on the BET surface area of MOF-5 after the 40% relative humidity exposure experiment (Figure S16, BET SA = 63 m^2/g). No amount of drying or gentle heating could recover the framework Ps signal.[48] PXRD of MOF-5 after the 40% relative humidity exposure shows obvious structural transformation (Figure S12). The change of MOF-5 crystallinity reveals that the framework collapses and transforms into ZnBDC·$x$$H_2O$ (BDC = benzene-1,4-dicarboxylate, where x is between 1 and 2) with little porosity.[39]

Repeating the above experiment with a relative humidity of 30%, the Ps intensity and Ps framework lifetime do not change after 200 h of exposure. The BET surface area of MOF-5 after 200 h of 30% relative humidity treatment (red symbols in Figure S16) is very close to that of initially activated MOF-5 (black symbols in Figure S16). After 43 h of exposure to 40% relative humidity, MOF-5 loses 99.5% of the framework pores, while no degradation is observed at 30% relative humidity. This difference in degradation behavior of MOF-5 under different humidities is not a dose effect. To illustrate this point, Ps intensity (%) is plotted against total H_2O charged per mass of MOF (g/g) (Figure S10). With 5.94 g of H_2O charged per gram of MOF-5 under a relative humidity of 40%, corresponding to 43 h of humidity treatment, the Ps intensity goes down to 0.15% (green symbols in Figure S10) indicating collapse of the lattice. Under a relative humidity of 30%, after a similar dose of H_2O charged per gram of MOF-5 (black symbols in Figure S10) which corresponds to 57.5 h of humidity treatment, the Ps intensity stays around 32%, and MOF-5 remains intact. Thus, relative humidity, not water dosage, is key to the water degradation process.

To more precisely define the region of stability for MOF-5, a series of relative humidities were explored, and the Ps intensity and Ps framework lifetimes collected. The framework intensities (Figure 3a) and framework Ps lifetimes (Figure S4) are plotted against flow time of the humid nitrogen with different relative humidities. For all cases, the framework pore size does not change significantly, the intensities of MOF-5 framework Ps follow a universal sigmoidal trend: the porosity reaches almost zero, and the water degradation of MOF-5 reaches completion. Therefore, an equilibrium water adsorption isotherm is not achievable for MOF-5 because the water adsorption of MOF-5 is irreversible. The shape of the MOF-5 water breakthrough curve[49] suggests that the water uptake is attributed to irreversible transformation. MOF-5 will eventually reach its completely degraded phase under any relevant humidity. The MOF-5 "half degradation time ($T_{1/2}$)" defined as the number of hours required for the framework intensity to decrease to half of its original value shows a nominally exponential dependence on relative humidity as shown in Figure 3b. Once the time factor is removed by plotting Ps

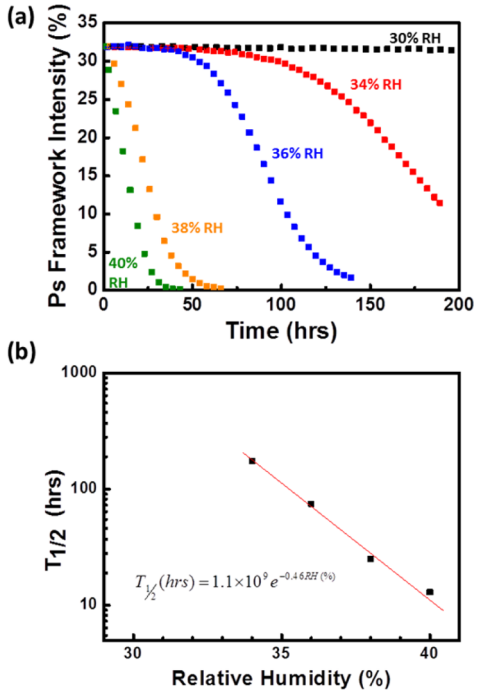

Figure 3. (a) Ps framework intensity of MOF-5 (Ps lifetime = 13.5 ns, pore diameter = 1.28 nm) against time (hours) under the relative humidities (RHs) of 30% (black), 34% (red), 36% (blue), 38% (orange), and 40% (green) at 25 °C. (b) The time required for the Ps framework intensity to decrease to half its starting value ($T_{1/2}$) as a function of relative humidity. Error bars are smaller than the plotting symbols.

DOI: 10.1021/ja512382f
J. Am. Chem. Soc. 2015, 137, 2651−2657

framework lifetime against framework intensity, the entire degradation processes coincide with each other (Figure S8). However, the lower the relative humidity, the longer time it takes for the Ps intensity to start to decay. It also shows that at 30% relative humidity, even after 189 h of exposure to humidity, the Ps intensity is hardly altered (black symbols in Figure 3), while for the same amount of time, at a slightly higher relative humidity (34%), the Ps intensity already decreases to 11.5%, which corresponds to 40% of the framework being damaged (red symbols in Figure 3). The results imply that how early the framework degradation happens depends on the concentration of water (i.e relative humidity of gas flow) in stark contrast to the typical methods of degradation for water sensitive metal complexes. The higher the relative humidity, the longer MOF-5 has been exposed to the humidity, and the larger the amount of water the framework has been exposed to, the faster degradation occurs and proceeds.

An induction period manifested in the initiation phase of the sigmoidal degradation curve has been discovered, suggesting a relative humidity window for long-term stability for MOF-5. To further test this hypothesis, additional experiments were conducted to assess the long-term stability of MOF-5. Little change in PXRD patterns is seen after 6 months of exposure to humid air with relative humidity up to 11% (Figure S21). This indicates that in applications such as hydrogen storage, where the water concentration would be low, moisture instability is not a concern for MOF-5. The gross morphology of the samples is observed to be unchanged. This finding runs counter to countless assertions in the literature which, though perhaps intuitive, do not have any long-term stability testing of relevance to support them.

There is a dramatic change in the stability of MOF-5 within a small window of relative humidity. Under a relative humidity of 36% (blue symbols in Figure 3a), the Ps intensity of MOF-5 framework was not observed to be reduced after 11 h because there are few hydrophilic groups present in the intact MOF-5: all the carboxylate groups are coordinatively bonded to Zn_4O^{6+} metal clusters. At longer times, the Ps intensity decreases slowly. The reduction of Ps intensity accelerates progressively as the degradation proceeds, and the amount of broken coordination bonds between linkers and metal clusters increases exposing more hydrophilic functional groups. This can be explained considering that the broken bonds from the decomposition reactions on the framework in turn promote the degradation of the crystal. Decomposition again slows down toward the end of the curve due to the shrinkage of the number of surviving hydrolysis-prone sites in the framework at the end of the curve.

In light of these observations, we hypothesized that other MOFs based on the basic Zn_4O cluster might also have regions of stability under humid conditions. UMCM-8 is composed of $Zn_4O(CO_2R)_6$ metal clusters and a 1:1 ratio of the linear linkers benzene-1,4-dicarboxylate (BDC) and naphthalene-2,6-dicarboxylate (NDC). It has a structure similar to MOF-5, but instead of having cubic cages of a single size, it has two cubic cages and two tetragonal cages (Figure 1) and larger voids than MOF-5. The larger the pores, the longer the Ps framework lifetime (less rapid the Ps annihilation) because of the reduced overlap of the Ps wave function with the surrounding electrons of the pore walls. It is generally observed, within a homologous series, that MOFs with larger void spaces display less stability due to a tendency toward structural collapse.[49] On this basis the larger pores of UMCM-8 might be expected to engender reduced stability toward water. However, the degradation of UMCM-8 in fact requires higher relative humidity than MOF-5 (Figure 4). At 36% relative humidity, conditions that can

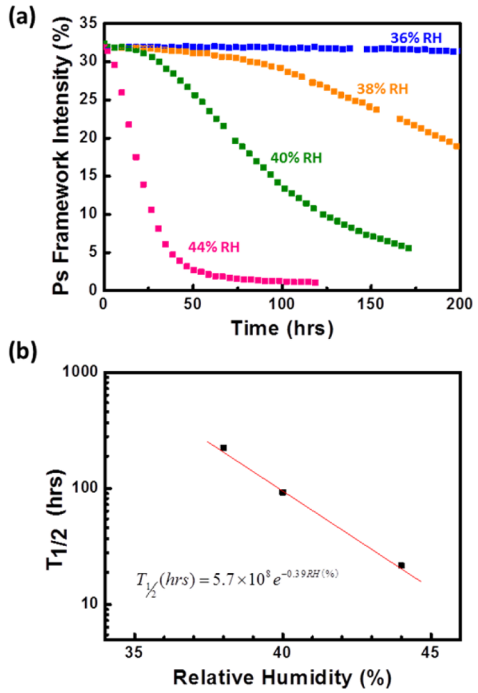

Figure 4. (a) Ps framework intensity of UMCM-8 (Ps lifetime = 16.0 ns, pore diameter = 1.40 nm) as a function of time under the relative humidities (RHs) of 36% (blue), 38% (orange), 40% (green), and 44% (pink) at 25 °C. (b) The correlation between half degradation time ($T_{1/2}$) of UMCM-8 and relative humidity. Error bars are smaller than the plotting symbols.

initiate the decomposition of MOF-5 do almost nothing to the Ps intensity (blue symbols in Figure 4) or Ps framework lifetime (Figure S5) in UMCM-8 for 200 h. The Ps framework lifetime of UMCM-8 remains at 16 ns which corresponds to an average pore diameter of 1.4 nm, and Ps intensity stays at 32% which corresponds to an intact framework. When the relative humidity is increased to 44%, the Ps framework lifetime drops from 16 to 12 ns in 120 h (pink symbols in Figure S5), and the Ps intensity shows a sigmoidal trend similar to MOF-5. These results imply that with the same concentration of water, MOFs with the same metal clusters but different pore sizes/hydrophilicity tolerate water vapor to different extent. In combination with recent studies demonstrating that more sterically demanding ligands improving kinetic stability toward humidity degradation,[24,50] this suggests a two-fold approach to overcoming water instability for this large class of MOFs. The proposed explanation for the greater stability of UMCM-8 is that the attack of water on the MOF does not happen through interaction of a single water molecule with a metal cluster breaking/disturbing the interaction of the Zn−O tetrahedron. The size of the pore and the hydrophilicity of linkers play important roles as well. The hypothesis is that degradation must be triggered by a certain amount of accumulation of water in the pore, a mechanism similar to capillary condensation. The larger the inner diameter of the pore, the higher the partial pressure of water (relative humidity of gas stream in the present case) is needed to accumulate sufficient water molecules to

DOI: 10.1021/ja512382f
J. Am. Chem. Soc. 2015, 137, 2651−2657

hydrolyze coordination bonds between linkers and metal ions. The hydrophilicity of linkers may also contribute to the stability difference between MOF-5 and UMCM-8. The computed log P (calculation see Supporting Information) value of benzene (1.97) is lower than that of naphthalene (2.96) which means that BDC is more hydrophilic than NDC. Even though a fraction of cages in UMCM-8 have the same size as MOF-5, UMCM-8 does not start degrading at the same time with MOF-5. This observation implies that the degradation of the series of Zn_4O-based MOFs does not start unless accumulation of water molecules takes place in multiple cages. Otherwise, UMCM-8 and MOF-5 should have started to decompose at the same relative humidity.

To further explore the factors dictating hydrolytic stability, the IRMOF $Zn_4O(FMA)_3$ was studied using the same approach with PALS under 30% relative humidity, and the results were compared to MOF-5 (Figure 5). This material, reported by

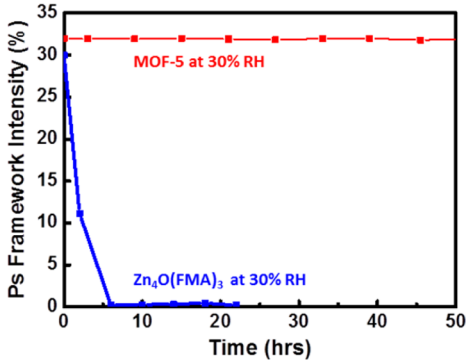

Figure 5. Comparison of Ps framework intensities between $Zn_4O(FMA)_3$ (blue, Ps lifetime = 8.9 ns, pore diameter = 1.05 nm), and MOF-5 (red) at 30% relative humidity (RH) at 25 °C. Error bars are smaller than the plotting symbols.

Chen and co-workers, is constructed from the $Zn_4O(CO_2R)_6$ metal clusters and fumarate linkers; it is among the smallest pore members of the IRMOF series. The log P value of ethene is 1.11 suggesting that fumarate is much less hydrophobic than either BDC or NDC. Moreover, with a theoretical cage side-length of 1.08 nm, $Zn_4O(FMA)_3$ is smaller than MOF-5 and therefore can shed light upon the issue of pore size in promoting decomposition (framework Ps lifetime of 8.9 ns vs 13.5 ns for MOF-5). In Figure 5, the framework porosity of $Zn_4O(FMA)_3$ is severely reduced under the conditions of 30% relative humidity: the Ps intensity decreases to 0% within 6 h, whereas MOF-5 shows almost no reduction in framework intensity even after 200 h under these conditions. The BET surface area of as-synthesized $Zn_4O(FMA)_3$ is 2009 m^2/g (previously reported: 1120 m^2/g; theoretical surface area: 2835 m^2/g, see Supporting Information), whereas after hydration, its BET surface area decreases to 30 m^2/g (Figure S18). Based on the fact that the Ps framework intensity of $Zn_4O(FMA)_3$ decreases by an absolute value of 1.7% after 45 h of 16% relative humidity treatment and keeps decreasing slowly with time, the relative humidity region of water stability for $Zn_4O(FMA)_3$ is much lower than that of MOF-5 and UMCM-8 (Figure S11). The comparison of the region of water stability for $Zn_4O(FMA)_3$, MOF-5, and UMCM-8 illustrates the range of different behaviors that can be seen for hydrocarbon linkers within the same basic coordination motif and suggests larger pores lead to greater resistance to hydrolysis.

The functionality of linkers can influence water stability of Zn_4O-based MOFs. Hydrophilic functional groups are expected to reduce water stability. Aniline, the core of the linker yielding IRMOF-3, has a log P of 1.14, a value lower than 1.97 for benzene due to the presence of the $-NH_2$ group. It has been reported that IRMOF-3 is more stable than MOF-5 in ambient air.[25] However, continuous monitoring of porosity by PALS indicates that IRMOF-3 is in fact more sensitive to humidity than MOF-5. Figure 6 plots the intensity of Ps annihilating

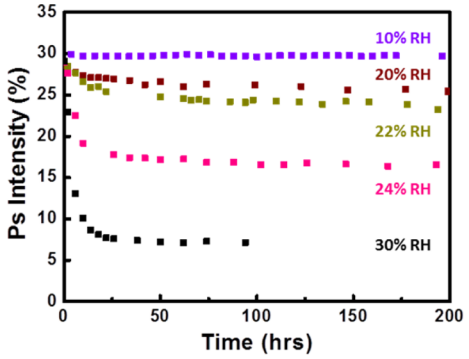

Figure 6. Ps intensity of IRMOF-3 (Ps lifetime = 10.3 ns, pore diameter = 1.12 nm) against time under the relative humidities (RHs) of 10% (violet), 20% (burgundy), 22% (dark yellow), 24% (pink), and 30% (black) at 25 °C. Error bars are smaller than the plotting symbols.

inside the IRMOF-3 crystals as a function of exposure time for various values of relative humidity. This intensity is the sum of the intensity of Ps annihilating in surviving pristine lattice (Ps lifetime = 8−10.3 ns) and the intensity of Ps (Ps lifetime = 13−28 ns) trapped in larger voids generated near regions of lattice collapse, representing all Ps annihilating inside the IRMOF-3 crystals. The fitted framework lifetime is reduced because of the additional effect of it disappearing into the intermediate component. At short exposure times, this trapped void component is impossible to resolve because its Ps lifetime is very close to the pristine lattice Ps lifetime and its intensity is very low. At long exposure times, this void component grows in to comprise ~2/3 of the (decaying) residual total intensity with lifetimes that range from 17 ns for 20% relative humidity to 28 ns for 30% relative humidity (corresponding to void diameters of 1.7 and 2.2 nm, respectively). The sum of intensities plotted in Figure 6 is robust and nominally corresponds to the relative residual porosity as plotted in Figures 3a and 4a.

The black symbols in Figure 6 shows that the Ps intensity of IRMOF-3 drops dramatically within 24 h of exposure to 30% relative humidity in a quasi-exponential fashion; this shape contrasts dramatically with the sigmoidal shapes seen in the MOF-5 and UMCM-8 experiments. The Ps intensity of IRMOF-3 then stabilizes around 7%. The differences in water stabilities and degradation trends between IRMOF-3 and MOF-5 are attributable to the fact that the linker of IRMOF-3, 2-aminoterephthalate, has a higher water affinity than the linker of MOF-5 and, perhaps more critically, the water-induced decomposition product of IRMOF-3 is amorphous, whereas it is crystalline for MOF-5. There is no apparent induction period for the degradation of IRMOF-3 exposed to 30% relative humidity. This suggests that the hydrophilic nature of the functional groups, and the perhaps even the participation of

DOI: 10.1021/ja512382f
J. Am. Chem. Soc. 2015, 137, 2651−2657

these groups in decomposition, eliminates the need for clusters of water molecules and existing framework damage. The rate of degradation decreases over time as a result of the loss in the number of intact pores, although the fact that the damage levels out suggests that the decomposition process is somewhat self-protective of inner porosity *vide infra*.

Under a lower relative humidity of 24%, the degradation of IRMOF-3 caused by water follows the same trend as described above, although the Ps intensity stabilizes at a higher level, around 16% after 70 h (pink symbols in Figure 6). Red symbols in Figure S24 show the relative intensity of the peak at 2θ = 6.86° in IRMOF-3 PXRD patterns changing with time under 30% relative humidity. The intensity of the primary PXRD peak at 2θ = 6.86° goes down quickly to 0.4% of the original intensity and then plateaus, which agrees with how the porosity changes based on Ps intensity information (black symbols in Figure S24). With a relative humidity of 24%, the intensity of the primary peak in IRMOF-3 PXRD patterns decreases and plateaus around 33% of the original intensity, which is in accord with Ps intensity trend as well (Figure S25). These experiments demonstrate that the porosity evolution is correlated with the evolution of crystallinity. This can be explained by a model wherein IRMOF-3 degrades into an amorphous phase with no new crystallinity appearing (Figure S15) and the amorphous continuous layer protects the interior crystalline material from further contact with water, a mechanism analogous to self-protective oxide formation in certain metals. In contrast to MOF-5, which transforms into another crystalline phase ($ZnBDC{\cdot}xH_2O$)[39] upon water exposure apparently with gaps for water to pass through and continue degradation the remaining MOF-5, IRMOF-3 acts differently upon encountering water. The observation of a preservation of the bulk crystal morphology of IRMOF-3 in previous studies[25] also supports a mechanism where protection by an amorphous layer for the IRMOF-3 prevents complete loss of crystallinity. All the curves asymptotically approach equilibrium framework intensities that are stable at the given relative humidities and are lower as the humidity increases.

Water sensitivity of MOFs is history dependent as well. Figure 7 shows that water-induced decomposition in MOFs leads to higher sensitivity to humidity. To illustrate this point, MOF-5 was treated for 100 h with 36% relative humidity at 20 mL/min until the Ps framework intensity decreased to 13% (a 60% reduction from the pristine material). The humidity was then decreased to 30%. Unlike the almost unchanged framework intensity of pristine MOF-5 treated with 30% relative humidity right from the beginning (black symbols in Figure 7), the framework intensity of damaged MOF-5 now decreases much more rapidly, at a rate of 0.068% Ps framework intensity per hour. This is slow compared to 0.49% per hour before the switch (Figure 7), but there is clearly no induction period at the 100 h turning point of relative humidity. This indicates that the defects created by water lead to faster degradation kinetics. In other words the history of the sample, in terms of previous exposure to moisture, influences the amount of defects in the MOF and therefore the time required for degradation at a given humidity.

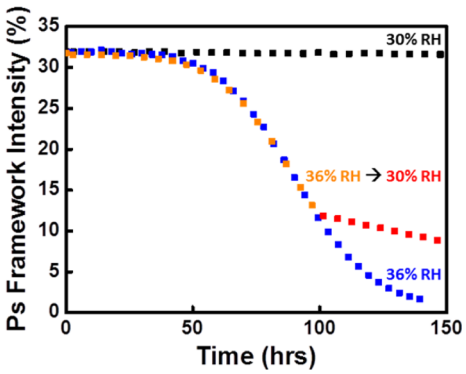

Figure 7. Ps framework intensity of MOF-5 against time under the relative humidities (RHs) of 36% (orange) and then 30% (red) at 25 °C. Ps framework intensities of MOF-5 under the relative humidity of only 36% (blue) and only 30% (black) are plotted for comparison. Error bars are smaller than the plotting symbols.

CONCLUSIONS

PALS incorporated within a flow-through system allows monitoring structural degradation of MOFs in real-time under dynamic humid conditions. For MOF-5 and UMCM-8, the evolution rate of porosity depends sensitively (exponentially) on relative humidity and proceeds by a universal sigmoidal decrease. This indicates that the damage mechanism(s) and evolution of structure are the same under different relative humidities. An induction period consistent with exponentially long MOF degradation has been revealed for a group of MOFs with $Zn_4O(CO_2R)_6$ metal clusters. Controlling the relative humidity, even over a fairly large and operationally relevant window, allows for long-term stability of these MOFs against water vapor. The water stability of Zn_4O-based MOFs with cubic structure was found to be related to pore size and linker hydrophilicity, as demonstrated by comparison of the behavior of UMCM-8, MOF-5, $Zn_4O(FMA)_3$, and IRMOF-3. These results deepen the understanding of the stability of MOFs against water and demonstrate that water stability is strongly dependent on relative humidity such that appropriate process parameters can be chosen for long-term stability in applications such as fuel gas storage, separations, and catalysis.

ASSOCIATED CONTENT

Supporting Information

Experimental details of MOF syntheses, PALS incorporated with flow-through system and experiments, theoretical correlation between Ps lifetime and pore diameter, comparison of PALS pore-size measurements with other methods, Ps lifetime spectra of MOF-5, initial activated and posthydration-PALS MOFs analyzed by PXRD and N_2 adsorption measurement, Ps framework intensity of MOF-5 as a function of total H_2O charged per MOF, Ps framework lifetime of MOF-5 as a function of time, Ps framework lifetime of UMCM-8 as a function of time, Ps framework lifetime of MOF-5 as a function of total H_2O charged per MOF, Ps framework lifetime of UMCM-8 as a function of total H_2O charged per MOF, Ps framework lifetime of MOF-5 as a function of Ps framework intensity, Ps framework lifetime of UMCM-8 as a function of Ps framework intensity, Ps framework intensity of $Zn_4O(FMA)_3$ as a function of time under 16% relative humidity, log P calculation, comparison of linker hydrophobicity, long-term water stability experiments of MOF-5, comparison between crystal structures of IRMOF-3 and MOF-5, the intensity of PXRD primary peak of IRMOF-3 as a function of time at 30% relative humidity, the intensity of PXRD primary peak of IRMOF-3 as a function of time at 24% relative humidity. This

DOI: 10.1021/ja512382f
J. Am. Chem. Soc. 2015, 137, 2651−2657

material is available free of charge via the Internet at http://pubs.acs.org.

AUTHOR INFORMATION

Corresponding Authors

*matzger@umich.edu
*gidley@umich.edu

Present Address

[§]Radiochemistry Division, Bhabha Atomic Research Centre, Trombay, Mumbai 400 085, India.

Notes

The authors declare no competing financial interest.

ACKNOWLEDGMENTS

We acknowledge Dr. William Frieze for PALS equipment support; Dr. Jeremy Feldblyum, Dr. Paolo Crivelli and Dr. Bernardo Barbiellini for helpful discussions; Laura Pfund and Jonathan Bennion for technical support; and James Imirzian for preliminary studies. Synthesis of materials and additional characterization were supported by the U.S. Department of Energy (DE-SC0004888) with the exception of PALS studies which were supported by the National Science Foundation (DMR-0907369).

REFERENCES

(1) Rosi, N. L.; Eckert, J.; Eddaoudi, M.; Vodak, D. T.; Kim, Jaheon; O'Keeffe, M.; Yaghi, O. M. *Science* **2003**, *300*, 1127−1129.
(2) Murray, L. J.; Dincă, M.; Long, J. R. *Chem. Soc. Rev.* **2009**, *38*, 1294−1314.
(3) Suh, M. P.; Park, H. J.; Prasad, T. K.; Lim, D.-W. *Chem. Rev.* **2012**, *112*, 782−835.
(4) Liu, Y.; Kabbour, H.; Brown, C. M.; Neumann, D. A.; Ahn, C. C. *Langmuir* **2008**, *24*, 4772−4777.
(5) Millward, A. R.; Yaghi, O. M. *J. Am. Chem. Soc.* **2005**, *127*, 17998−17999.
(6) Matzger, A. J.; Wong-Foy, A. G. Caskey, S. Microporous coordination polymers as novel sorbents for gas separation. US20100258004 A1, October 14, 2010.
(7) Bloch, E. D.; Queen, W. L.; Krishna, R.; Zadrozny, J. M.; Brown, C. M.; Long, J. R. *Science* **2012**, *335*, 1606−1610.
(8) Dietzel, P. D. C.; Besikiotis, V.; Blom, R. *J. Mater. Chem.* **2009**, *19*, 7362−7370.
(9) Lin, L.-C.; Kim, J.; Kong, X.; Scott, E.; McDonald, T. M.; Long, J. R.; Reimer, J. A.; Smit, B. *Angew. Chem., Int. Ed.* **2013**, *52*, 4410−4413.
(10) Cychosz, K. A.; Wong-Foy, A. G.; Matzger, A. J. *J. Am. Chem. Soc.* **2009**, *131*, 14538−14543.
(11) Cychosz, K. A.; Ahmad, R.; Matzger, A. J. *Chem. Sci.* **2010**, *1*, 293−302.
(12) Li, J.-R.; Kuppler, R. J.; Zhou, H.-C. *Chem. Soc. Rev.* **2009**, *38*, 1477−1504.
(13) Lee, J.; Farha, O. K.; Roberts, J.; Scheidt, K. A.; Nguyen, S. T.; Hupp, J. T. *Chem. Soc. Rev.* **2009**, *38*, 1450−1459.
(14) Schoenecker, P. M.; Carson, C. G.; Jasuja, H.; Flemming, C. J. J.; Walton, K. S. *Ind. Eng. Chem. Res.* **2012**, *51*, 6513−6519.
(15) Küsgens, P.; Rose, M.; Senkovska, I.; Fröde, H.; Henschel, A.; Siegle, S.; Kaskel, S. *Microporous Mesoporous Mater.* **2009**, *120*, 325−330.
(16) Cavka, J. H.; Jakobsen, S.; Olsbye, U.; Guillou, N.; Lamberti, C.; Bordiga, S.; Lillerud, K. P. *J. Am. Chem. Soc.* **2008**, *130*, 13850−13851.
(17) Demessence, A.; D'Alessandro, D. M.; Foo, M. L.; Long, J. R. *J. Am. Chem. Soc.* **2009**, *131*, 8784−8786.
(18) Canivet, J.; Fateeva, A.; Guo, Y.; Coasne, B.; Farrusseng, D. *Chem. Soc. Rev.* **2014**, *43*, 5594−5617.
(19) Burtch, N. C.; Jasuja, H.; Walton, K. S. *Chem. Rev.* **2014**, *114*, 10575−10612.
(20) Qadir, N. ul; Said, S. A. M.; Bahaidarah, H. M. *Microporous Mesoporous Mater.* **2015**, *201*, 61−90.
(21) Cychosz, K. A.; Matzger, A. J. *Langmuir* **2010**, *26*, 17198−17202.
(22) Low, J. J.; Benin, A. I.; Jakubczak, P.; Abrahamian, J. F.; Faheem, S. A.; Willis, R. R. *J. Am. Chem. Soc.* **2009**, *131*, 15834−15842.
(23) Klinowski, J.; Paz, F. A. A.; Silva, P.; Rocha, J. *Dalton Trans.* **2010**, *40*, 321−330.
(24) Yang, J.; Grzech, A.; Mulder, F. M.; Dingemans, T. J. *Chem. Commun.* **2011**, *47*, 5244−5246.
(25) Nguyen, J. G.; Cohen, S. M. *J. Am. Chem. Soc.* **2010**, *132*, 4560−4561.
(26) Decoste, J. B.; Peterson, G. W.; Smith, M. W.; Stone, C. A.; Willis, C. R. *J. Am. Chem. Soc.* **2012**, *134*, 1486−1489.
(27) Zhang, W.; Hu, Y.; Ge, J.; Jiang, H.-L.; Yu, S.-H. *J. Am. Chem. Soc.* **2014**, *136*, 16978−16981.
(28) Feldblyum, J. I.; Liu, M.; Gidley, D. W.; Matzger, A. J. *J. Am. Chem. Soc.* **2011**, *133*, 18257−18263.
(29) Xue, M.; Liu, Y.; Schaffino, R. M.; Xiang, S.; Zhao, X.; Zhu, G.-S.; Qiu, S.-L.; Chen, B. *Inorg. Chem.* **2009**, *48*, 4649−4651.
(30) Li, H.; Eddaoudi, M.; O'Keeffe, M.; Yaghi, O. M. *Nature* **1999**, *402*, 276−279.
(31) Koh, K.; Van Oosterhout, J. D.; Roy, S.; Wong-Foy, A. G.; Matzger, A. J. *Chem. Sci.* **2012**, *3*, 2429−2432.
(32) Rowsell, J. L. C.; Yaghi, O. M. *J. Am. Chem. Soc.* **2006**, *128*, 1304−1315.
(33) Gidley, D. W.; Peng, H.-G.; Vallery, R. S. *Annu. Rev. Mater. Res.* **2006**, *36*, 49−79.
(34) Jean, Y. C.; Van Horn, J. D.; Hung, W.-S.; Lee, K.-R. *Macromolecules* **2013**, *46*, 7133−7145.
(35) Liu, M.; Wong-Foy, A. G.; Vallery, R. S.; Frieze, W. E.; Schnobrich, J. K.; Gidley, D. W.; Matzger, A. J. *Adv. Mater.* **2010**, *22*, 1598−1601.
(36) Feldblyum, J. I.; Dutta, D.; Wong-Foy, A. G.; Dailly, A.; Imirzian, J.; Gidley, D. W.; Matzger, A. J. *Langmuir* **2013**, *29*, 8146−8153.
(37) Tao, S. J. *J. Chem. Phys.* **1972**, *56*, 5499−5510.
(38) Eldrup, M.; Lightbody, D.; Sherwood, J. N. *Chem. Phys.* **1981**, *63*, 51−58.
(39) Hausdorf, S.; Wagler, J.; Mossig, R.; Mertens, F. O. R. L. *J. Phys. Chem. A* **2008**, *112*, 7567−7576.
(40) Wong-Foy, A. G.; Matzger, A. J.; Yaghi, O. M. *J. Am. Chem. Soc.* **2006**, *128*, 3494−3495.
(41) Park, T.-H.; Hickman, A. J.; Koh, K.; Martin, S.; Wong-Foy, A. G.; Sanford, M. S.; Matzger, A. J. *J. Am. Chem. Soc.* **2011**, *133*, 20138−20141.
(42) Greathouse, J. A.; Allendorf, M. D. *J. Am. Chem. Soc.* **2006**, *128*, 10678−10679.
(43) Sabo, M.; Henschel, A.; Fröde, H.; Klemm, E.; Kaskel, S. *J. Mater. Chem.* **2007**, *17*, 3827−3832.
(44) Schröck, K.; Schröder, F.; Heyden, M.; Fischer, R. A.; Havenith, M. *Phys. Chem. Chem. Phys.* **2008**, *10*, 4732−4739.
(45) Yang, S. J.; Choi, J. Y.; Chae, H. K.; Cho, J. H.; Nahm, K. S.; Park, C. R. *Chem. Mater.* **2009**, *21*, 1893−1897.
(46) Chen, X.; Lukaszczuk, P.; Tripisciano, C.; Rümmeli, M. H.; Srenscek-Nazzal, J.; Pelech, I.; Kalenczuk, R. J.; Borowiak-Palen, E. *Phys. Status Solidi B* **2010**, *247*, 2664−2668.
(47) Kaye, S. S.; Dailly, A.; Yaghi, O. M.; Long, J. R. *J. Am. Chem. Soc.* **2007**, *129*, 14176−14177.
(48) However, a new Ps lifetime of 2 ns is observed in the new structure after drying. This indicates that there is some ultra-microporosity around 0.5 nm, which is in consistent with the formation of a new structure type.
(49) Guo, P.; Wong-Foy, A. G.; Matzger, A. J. *Langmuir* **2014**, *30*, 1921−1925.
(50) Farha, O. K.; Hupp, J. T. *Acc. Chem. Res.* **2010**, *43*, 1166−1175.
(51) Jasuja, H.; Huang, Y.; Walton, K. S. *Langmuir* **2012**, *28*, 16874−16880.

DOI: 10.1021/ja512382f
J. Am. Chem. Soc. 2015, 137, 2651−2657